Receptor sequestration in response to β-arrestin-2 phosphorylation by ERK1/2 governs steady-state levels of GPCR cell-surface expression

Justine S. Paradis[a], Stevenson Ly[a,b], Élodie Blondel-Tepaz[a], Jacob A. Galan[a,c,1], Alexandre Beautrait[a], Mark G. H. Scott[d], Hervé Enslen[d], Stefano Marullo[d], Philippe P. Roux[a,c,2], and Michel Bouvier[a,b,2]

[a]Institute for Research in Immunology and Cancer, Université de Montréal, Montréal, QC H3C 1J4, Canada; [b]Department of Biochemistry and Molecular Medicine, Université de Montréal, Montréal, QC H3C IJ4, Canada; [c]Department of Pathology and Cell Biology, Université de Montréal, Montréal, QC H3C IJ4, Canada; and [d]Institut Cochin, Inserm U1016, CNRS UMR8104, Université Paris Descartes, Sorbonne Paris Cité, 75014 Paris, France

Edited by Solomon H. Snyder, Johns Hopkins University School of Medicine, Baltimore, MD, and approved August 13, 2015 (received for review May 5, 2015)

MAPKs are activated in response to G protein-coupled receptor (GPCR) stimulation and play essential roles in regulating cellular processes downstream of these receptors. However, very little is known about the reciprocal effect of MAPK activation on GPCRs. To investigate possible crosstalk between the MAPK and GPCRs, we assessed the effect of ERK1/2 on the activity of several GPCR family members. We found that ERK1/2 activation leads to a reduction in the steady-state cell-surface expression of many GPCRs because of their intracellular sequestration. This subcellular redistribution resulted in a global dampening of cell responsiveness, as illustrated by reduced ligand-mediated G-protein activation and second-messenger generation as well as blunted GPCR kinases and β-arrestin recruitment. This ERK1/2-mediated regulatory process was observed for GPCRs that can interact with β-arrestins, such as type-2 vasopressin, type-1 angiotensin, and CXC type-4 chemokine receptors, but not for the prostaglandin F receptor that cannot interact with β-arrestin, implicating this scaffolding protein in the receptor's subcellular redistribution. Complementation experiments in mouse embryonic fibroblasts lacking β-arrestins combined with in vitro kinase assays revealed that β-arrestin-2 phosphorylation on Ser14 and Thr276 is essential for the ERK1/2-promoted GPCR sequestration. This previously unidentified regulatory mechanism was observed after constitutive activation as well as after receptor tyrosine kinase- or GPCR-mediated activation of ERK1/2, suggesting that it is a central node in the tonic regulation of cell responsiveness to GPCR stimulation, acting both as an effector and a negative regulator.

β-arrestin | MAPK | G protein-coupled receptor | internalization | cell signaling

The ERK/MAPK pathway (1, 2) traditionally has been linked to the activation of receptor tyrosine kinases (RTKs) (3, 4), but in recent years, G protein-coupled receptor (GPCR)-mediated ERK/MAPK activation also has been shown to play important roles (5). Such convergence on the ERK/MAPK signaling module generates multiple opportunities for regulating crosstalk between GPCR and RTK signaling, and many distinct molecular mechanisms have been described (6). GPCRs activate the ERK/MAPK pathway via both G protein-dependent (canonical) and -independent (noncanonical) pathways. The canonical pathway can involve diverse Gα and/or Gβγ subunits that cause ERK1/2 activation through various downstream effectors, such as PI3K and exchange protein directly activated by cAMP (EPAC), as well as PKA and PKC (7–11). Among the noncanonical mechanisms, engagement of β-arrestins (βarrs) scaffolding the ERK/MAPK module has attracted considerable attention (12–14). For both canonical (15) and noncanonical (16, 17) pathways, transactivation of RTKs downstream of some GPCRs also has been shown to contribute to ERK1/2 regulation. Particularly, direct recruitment of βarrs to several RTKs (18), including insulin-like growth factor receptor (IGFR) (19, 20), insulin receptor (IR) (21), and epidermal growth factor receptor (EGFR) (22–24), following activation of either RTK or GPCR also results in ERK1/2 activation, emphasizing the central role of βarrs in controlling ERK1/2 activity.

For classical G protein-mediated signaling, several processes controlling the duration of the signal have been elucidated, including both homologous and heterologous desensitizations. The former involves phosphorylation of the activated receptor by GPCR kinases (GRKs) leading to the high-affinity binding of βarrs to the activated receptor, uncoupling of the receptor from G proteins, and subsequent internalization (25–27). Heterologous desensitization occurs upon activation of second messenger-dependent kinases such as PKA or PKC and may or may not be followed by receptor internalization (28, 29). Although, as mentioned above, ERK1/2 activation now is recognized as a main signaling module in both G protein- and βarr-dependent pathways, very little is known about the possible adaptive mechanisms resulting from the activation of these kinases. In one study (30), phosphorylation of βarr1, but not βarr2, by ERK1/2 was proposed to inhibit the agonist-promoted translocation of βarr1 to the β2-adrenergic receptor, preventing its endocytosis. More recently, ERK1/2-promoted phosphorylation of rat βarr2 was shown to stabilize the complex between the B2-bradykinin

Significance

ERK1/2 are important G protein-coupled receptor (GPCR) signaling effectors, but their role as possible GPCR regulators remains largely uncharted. We report that ERK1/2 activation leads to the phosphorylation of β-arrestin-2 on Ser14 and Thr276, promoting the intracellular sequestration of unliganded GPCRs. This subcellular redistribution results in the dampening of cell responsiveness to GPCRs' ligand-mediated activation, positioning ERK1/2 as both a downstream effector and a negative regulator of GPCRs. Because ERK1/2 also is stimulated by receptor tyrosine kinases and is deregulated in many diseases, and because GPCRs respond to a large number of hormones and neurotransmitters, this newly uncovered regulatory process is poised to play a central role in controlling cell responsiveness in health and disease.

Author contributions: J.S.P., S.L., É.B.-T., J.A.G., A.B., M.G.H.S., H.E., S.M., P.P.R., and M.B. designed research; J.S.P., S.L., É.B.-T., J.A.G., A.B., and P.P.R. performed research; J.S.P., S.L., É.B.-T., J.A.G., A.B., M.G.H.S., H.E., S.M., P.P.R., and M.B. analyzed data; and J.S.P., P.P.R., and M.B. wrote the paper.

The authors declare no conflict of interest.

This article is a PNAS Direct Submission.

[1]Present address: Department of Molecular Biology, Massachusetts General Hospital, Boston, MA 02114.

[2]To whom correspondence may be addressed. Email: philippe.roux@umontreal.ca or michel.bouvier@umontreal.ca.

This article contains supporting information online at www.pnas.org/lookup/suppl/doi:10.1073/pnas.1508836112/-/DCSupplemental.

receptor and βarr2, thereby slowing the recycling of the receptor to the plasma membrane after agonist-promoted endocytosis (31). Although these data point to possible feedback roles for the ERK/MAPK pathway in receptor trafficking, they also raise important questions about the general role that ERK1/2 activation may play in GPCR activity.

Here we investigated the influence of ERK1/2 activation on GPCR responsiveness using the chemokine CXC type-4 receptor (CXCR4) as a model. We found that activation of the ERK/MAPK pathway results in decreased CXCR4 signaling upon stimulation by its native agonist, CXC type-12 (CXCL12). This reduced responsiveness resulted from the direct phosphorylation of βarr2 by ERK1/2 on two Ser/Thr residues, ultimately leading to the constitutive intracellular redistribution of the receptor. This previously unidentified regulatory mechanism is not restricted to CXCR4 and is shared by other GPCRs that are able to interact with βarrs. Our study therefore unravels an adaptive mechanism leading to a general dampening of cell responsiveness to GPCR stimulation in response to the activation of the ERK/MAPK by either RTKs or GPCRs.

Results

Activation of the ERK/MAPK Pathway Decreases CXCR4 Agonist-Induced Gi Activation. Gi protein activation downstream of agonist (CXCL12) stimulation of CXCR4 was examined in the presence or absence of upstream modulators of the ERK/MAPK pathway. G protein activation was monitored using an assay based on bioluminescence resonance energy transfer (BRET)

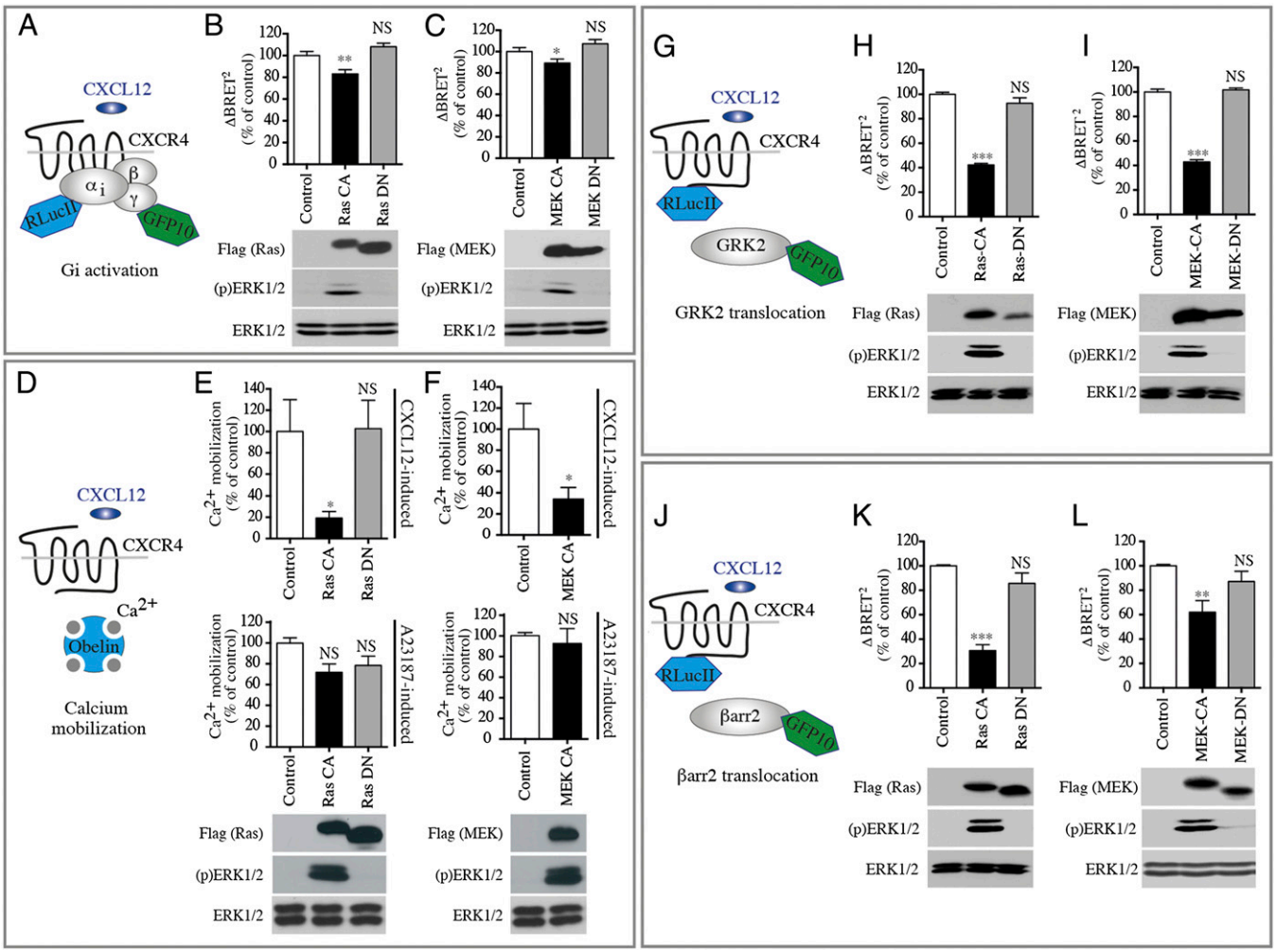

Fig. 1. ERK/MAPK pathway activation reduces Gi activation and second-messenger production as well as GRK2 and βarr2 translocation in response to CXCR4 activation. (*A*) Schematic representation of the BRET-based ligand-induced Gi activation assay. (*B* and *C*) CXCL12-promoted Gi activation measured by BRET in HEK293T cells cotransfected with HA-CXCR4, $G\alpha i_1$-RLucII, $G\beta_1$, and $G\gamma_2$-GFP10, without (Control) or with either Flag-Ras CA or Flag-Ras DN (*B*) or Flag-MEK CA or Flag-MEK DN (*C*). BRET400-GFP10 between $G\alpha i_1$-RLucII and $G\gamma_2$-GFP10 was measured after the addition of coel-400a, 3 min following the addition of CXCL12. Data are expressed as agonist-promoted BRET (ΔBRET; see Fig. S1*A*). (*D*) Schematic representation of the Obelin-based Ca^{2+} mobilization assay. (*E* and *F*) The increase in CXCL12-promoted intracellular calcium measured in HEK293T cells transfected with Obelin-Cherry in the absence (Control) or presence of the indicated Ras and MEK mutants. Luminescence was measured every second for 60 s after the injection of CXCL12 or calcium ionophore A23187. Bars represent the area under the curve calculated from the kinetics curves (Fig. S1*B*). (*G* and *J*) Schematic representations of the BRET-based ligand-induced GRK2 (*G*) and βarr2 (*J*) translocation. (*H*, *I*, *K*, and *L*) CXCL12-promoted BRET was measured in HEK293T cells transfected with CXCR4-RLucII and GRK2-GFP10 (*H* and *I*) or βarr2-GFP10 (*K* and *L*), in the absence (Control) or presence of the indicated Ras or MEK mutants. BRET400-GFP10 between CXCR4-RLucII and GRK2-GFP10 or βarr2-GFP10 was measured after the addition of coel-400a, 15 min after the addition of CXCL12. Data are expressed as agonist-promoted BRET (ΔBRET; see Fig. S1 *C* and *D*). In all cases, data shown represent the mean ± SEM of three independent experiments and were normalized to 100% of the control condition. Expression of CA or DN forms of Flag-Ras or Flag-MEK and the total ERK1/2 and ERK1/2 activation status [(p)ERK1/2], was assessed by immunoblotting. Representative experiments are shown below the graphs.*$P < 0.05$; **$P < 0.01$; ***$P < 0.001$; NS, not significant.

that detects the agonist-promoted separation of $G\alpha_{i1}$ and $G\gamma_2$ in intact cells (Fig. 1*A*) (32). CXCL12 induces a rapid decrease in BRET signal between $G\alpha_{i1}$-91RLucII and GFP10-$G\gamma_2$ in cells coexpressing the unmodified CXCR4 and $G\beta_1$ (Fig. S1*A*). Constitutively active (CA) forms of H-Ras [Ras-CA (Ras-G12V)] and MAPK/ERK kinase 1 (MEK1) [MEK-CA (MEK-S218/222D)], which promote ERK1/2 activation (33), diminished CXCL12-induced activation of Gi compared with cells expressing an empty vector or the dominant-negative (DN) forms of H-Ras [Ras-DN (Ras-S17N)] and MEK1 [MEK-DN (MEK-K97A)] (Fig. 1 *B* and *C*). Subsequently the effect of modulating the ERK/MAPK pathway on the CXCL12-evoked calcium response was examined using the Obelin biosensor (34) as a calcium reporter in HEK293T cells that endogenously express low levels of CXCR4 (Fig. 1*D* and Fig. S1*B*). The expression of both Ras-CA and MEK-CA reduced CXCL12-induced calcium mobilization, but Ras-DN did not (Fig. 1 *E* and *F*). In contrast, calcium mobilization triggered by the calcium ionophore A23187 was unaffected by modulation of the ERK/MAPK pathway (Fig. 1 *E* and *F*), indicating that CXCR4-dependent signaling is selectively reduced by activated ERK1/2. Because CXCR4-mediated calcium mobilization is a Gi-dependent response (35, 36), these findings demonstrate that activation of the ERK/MAPK pathway significantly reduces Gi activation and downstream calcium signaling upon CXCR4 stimulation. The larger reduction in the calcium response compared with the Gi activation signal most likely reflects the different assay modes (i.e., the greater number of spare receptors in the BRET-based Gi activation assay that requires exogenous CXCR4 coexpression).

Activation of the ERK/MAPK Pathway Decreases Agonist-Induced GRK2 and βarr2 Translocation. To investigate further the effect of ERK1/2 activation on CXCR4 signaling, we assessed CXCL12-promoted GRK2 and βarr2 translocation by BRET using CXCR4-RLucII and either GRK2-GFP10 or βarr2-GFP10 constructs (Fig. 1 *G* and *J* and Fig. S1 *C* and *D*). Coexpression of Ras-CA and MEK-CA, but not Ras-DN and MEK-DN, decreased the translocation of GRK2 and βarr2 following CXCR4 stimulation (Fig. 1 *H*, *I*, *K*, and *L*). Thus, in addition to blunting Gi responses, activation of the ERK/MAPK pathway greatly reduces GRK2 and βarr2 translocation.

ERK1/2 Activation Decreases CXCR4 Localization at the Cell Surface. The decrease in Gi activation and the reduced translocation of GRK2 and βarr2 could result either from a general loss of the receptor's ability to respond productively to CXCL12 or from a reduced number of receptors at the cell surface. To test the latter possibility directly, we assessed the effect of stimulating the ERK/MAPK pathway on CXCR4 cell-surface expression by dual-flow cytometry (dual FACS). This approach allows the measurement of cell-surface receptor density (reflected by HA immunoreactivity) as a function of total receptor number [reflected by the venus YFP (vYFP) fluorescence] in unpermeabilized HEK293T cells stably expressing HA-CXCR4-vYFP (Fig. 2*A*). Using this system, we found that Ras-CA and MEK-CA, but not Ras-DN and MEK-DN, led to a 70% reduction in the number of CXCR4 at the cell surface (Fig. 2 *B* and *C*).

To validate these findings further, we imaged the distribution of CXCR4-YFP by confocal fluorescence microscopy in HeLa cells. As shown in Fig. 3*A*, in the absence of ERK/MAPK activation, CXCR4 is localized mainly at the cell surface. Expression of either Ras-CA (Fig. 3*B*) or MEK-CA (Fig. 3*D*) resulted in a substantial loss of cell-surface receptors and the appearance of a punctate intracellular fluorescence signal indicating that activation of the ERK/MAPK pathway triggers the redistribution of CXCR4 to intracellular vesicles. The DN forms of Ras and MEK were without effect on CXCR4 distribution (Fig. 3 *C* and *E*). Semiquantification of the receptor redistribution using ImageJ

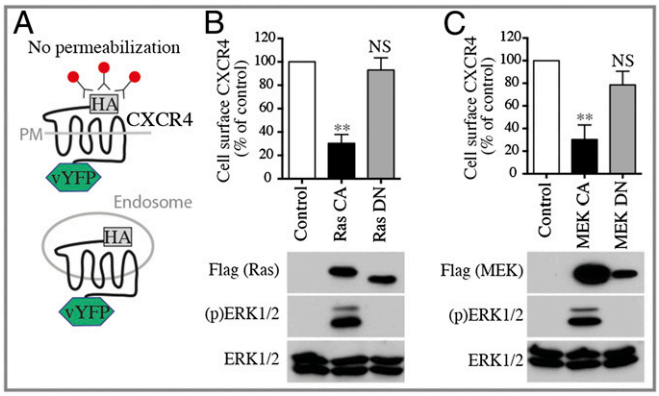

Fig. 2. Activation of the ERK/MAPK pathway reduces cell-surface expression of CXCR4. (*A*) Schematic representation of the receptor cell-surface expression assay. PM, plasma membrane. (*B* and *C*) Cell-surface CXCR4 levels were detected in HEK293T cells stably expressing HA-CXCR4-vYFP transfected without (Control) or with the indicated Ras and MEK mutants. Cells were labeled with a primary anti-HA and secondary Alexa 647-coupled chicken anti-mouse IgG antibodies, without permeabilization. Cell-surface expression of HA-CXCR4-vYFP in the absence of CXCL12 stimulation was measured by dual-flow cytometry. vYFP emission represents CXCR4 total expression; Alexa Fluor 647 emission represents CXCR4 plasma membrane expression. The relative cell-surface expression (the ratio of Alexa:vYFP mean emissions) is calculated from the YFP^+ cell population and is expressed as a percentage of the control condition. Data shown represent the mean ± SEM of three independent experiments. Expression of CA or DN forms of Flag-Ras or Flag-MEK and total ERK and ERK1/2 activation status [(p)ERK1/2] was assessed by immunoblotting. Representative experiments are shown below the graphs. $^{**}P < 0.01$; NS, not significant.

software (37) was performed by selecting transversal sections of the cells that allow definition of the plasma membrane and intracellular compartment (Fig. 3, *Right*). These data (Fig. S2) support the FACS results demonstrating that activation of the ERK/MAPK pathway promotes a significant subcellular redistribution of CXCR4 from the cell surface to the intracellular compartment.

Acute Stimulation of the ERK/MAPK Pathway Results in CXCR4 Intracellular Sequestration and Blunted Signaling. Next, we evaluated the effects of pharmacological and endogenous agonists of the ERK/MAPK pathway (38, 39) on the subcellular distribution and signaling capacity of CXCR4. Acute stimulation with phorbol 12-myristate 13-acetate (PMA) or EGF resulted in a weaker CXCL12-promoted recruitment of βarr2 (Fig. 4*A*) and an ~ 20% reduction in the proportion of cell-surface receptors in the absence of agonist stimulation (Fig. 4*B*). Interestingly, the kinetics of surface-receptor loss paralleled that of ERK1/2 activation, being transient with EGF stimulation and sustained with PMA stimulation, peaking at 15 or 30 min, respectively (Fig. 4*C*). Stimulation of the vasopressin type-2 receptor (V2R), a GPCR known to activate ERK1/2 strongly (40), also was found to induce CXCR4 sequestration to the same extent as EGF and PMA stimulation (Fig. 4*D*). In all cases, inhibition of ERK1/2 activation with the selective MEK1/2 inhibitor PD184352 (41) restored the initial proportion of cell-surface CXCR4 confirming that ERK1/2 activation is functionally correlated with the loss of cell-surface receptors. The effect of EGF stimulation on cell-surface receptors also was tested in the T-lymphoid cell line SUP-T1 that endogenously expresses CXCR4 (Fig. 4*E*). Indeed, FACS analysis using a monoclonal antibody directed against the extracellular domain of the human CXCR4 showed a significant EGF-evoked loss of cell-surface CXCR4, indicating that this modulation also is observed with endogenous receptors. Taken together, these data indicate that both acute and sustained stimulation of the ERK1/2

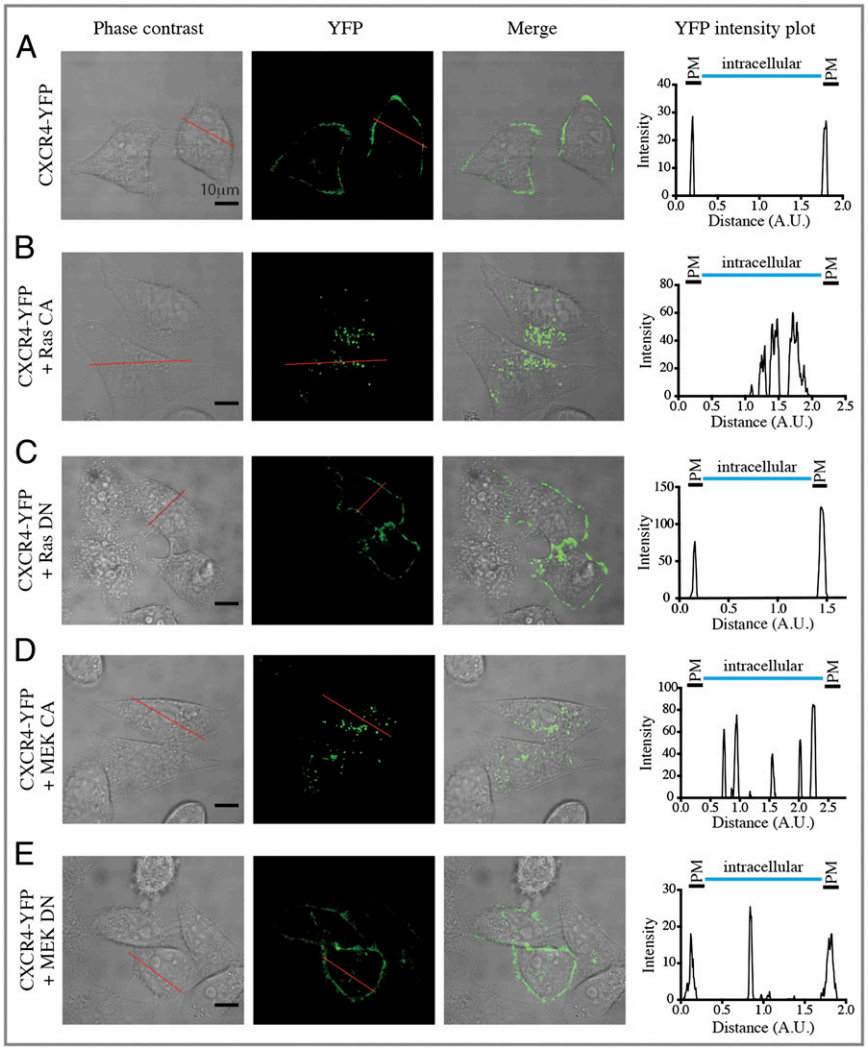

Fig. 3. Activation of the ERK/MAPK pathway leads to the redistribution of CXCR4 into intracellular vesicles (sequestration). CXCR4-YFP localization was assessed by fluorescence confocal microscopy in HeLa cells transfected with CXCR4-YFP without (*A*) or with (*B–E*) the indicated Ras (*B* and *C*) and MEK (*D* and *E*) mutants. (Scale bars, 10 μm.) Intensity as a function of the distance along a selected transversal section (red bar) was assessed using ImageJ software. Plots generated from phase-contrast images were used to identify the coordinates of the plasma membrane (PM) and the intracellular compartment of the cell. These coordinates are schematically indicated above the YFP intensity plots. Data shown are representative of more than 20 cells obtained from three independent experiments. Quantifications are presented in Fig. S2. A.U., arbitrary units.

signaling pathway promote CXCR4 redistribution, but, as would be expected, long-lasting activation results in more dramatic effects, reaching as much as 70% in the 48 h following the expression of constitutively active Ras and MEK mutants.

The ERK/MAPK Pathway Negatively Modulates Several GPCRs. Our results indicate that cell-surface CXCR4 density is negatively regulated upon activation of ERK1/2 by several agonists and in different cell types. To determine whether this regulatory mechanism can be generalized to other GPCRs, we assessed the effect of MEK-CA on three additional GPCRs, the vasopressin (V2R), the angiotensin (AT1R), and the prostaglandin (FP) receptors. To do so, we monitored G protein-mediated signaling, GRK2 and βarr2 recruitment, and cell-surface density. As shown in Fig. 5 *A* and *B*, we found that expression of MEK-CA, but not MEK-DN, led to a reduction in V2R and AT1R surface density. This loss of cell-surface receptors (60% for the V2R and 80% for the AT1R) resulted in diminished agonist-promoted recruitment of GRK2 and βarr2 as well as a blunted signaling response (cAMP production for V2R and Ca^{2+} mobilization for AT1R). The extent of signal reduction differed between the two receptors, probably reflecting distinct levels of coupling efficiency and spare receptors for the signaling pathways considered. No such negative regulation was observed for the FP receptor (Fig. 5*C*, *Left* and *Right*), indicating that only certain GPCRs are negatively regulated by ERK1/2. Interestingly, unlike CXCR4, V2R, and AT1R, the agonist stimulation of the FP receptor does not promote βarr2 translocation to the receptor (42) (Fig. 5*C*, *Center*), suggesting that the ERK1/2-dependent regulatory process may involve βarr2.

β-Arrestin Is Required for the ERK1/2-Dependent Cellular Redistribution of GPCRs. To confirm the role of βarr2 in the subcellular redistribution of CXCR4 in response to ERK1/2 activation, we analyzed CXCR4 cell-surface expression in mouse embryonic fibroblasts (MEFs) derived from WT and βarr1/2-KO animals (43). As was consistent with our observations in HEK293T, HeLa, and SupT1 cells, we found that activation of ERK1/2 led to a significant decrease in the proportion of CXCR4 at the cell surface in WT MEFs (Fig. 6*A*). Notably, this modulation was lost completely in βarr1/2-KO MEFs (Fig. 6*A*). Reintroducing βarr2 or βarr1 (Fig. 6*B*) in βarr1/2-KO MEFs by transfection restored the ERK1/2-promoted loss of cell-surface CXCR4, resulting in the sequestration of 30 ± 3% and 38 ± 4%, respectively, compared with 52 ± 4% for the WT MEFs. Coexpression of both βarr1 and βarr2 did not lead to a statistically significant greater loss of receptors (42 ± 5%), indicating that both βarr1 and βarr2 can promote receptor redistribution following ERK1/2 activation. Similar to observations in other cell types, expression of Ras-DN did not affect CXCR4 cell-surface density in βarr1/2-KO MEFs whether βarr2 was reintroduced or not (Fig. 6*C*), confirming the selectivity of action of active Ras.

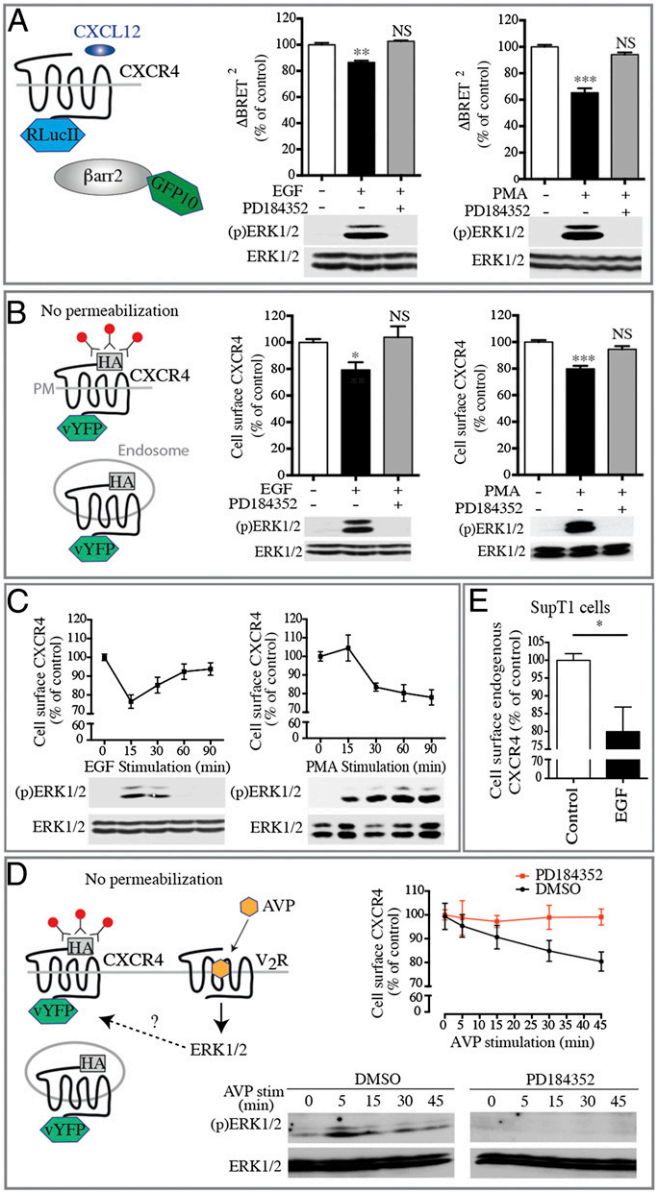

Fig. 4. Acute pharmacological activation of the ERK/MAPK pathway blunts CXCR4 signaling by reducing receptor cell-surface localization. (*A*) CXCL12-promoted βarr2 translocation is measured by BRET in HEK293T cells transfected with CXCR4-RLucII and βarr2-GFP10. Cells were pretreated with PD184352 for 30 min before stimulation with EGF for 15 min or with PMA for 30 min. BRET400-GFP10 between CXCR4-RLucII and βarr2-GFP10 was measured after the addition of coel-400a, 15 min following the addition of CXCL12. (*B*) CXCR4 cell-surface expression levels were assessed by dual-flow cytometry in HEK293T cells stably expressing HA-CXCR4-vYFP that were pretreated or not with PD184352 for 30 min before stimulation with EGF for 15 min or with PMA for 30 min. (*C*) Kinetics of CXCR4 cell-surface level reduction and ERK1/2 activation following EGF or PMA treatments. (*D*) Kinetics of the reduction of CXCR4 cell-surface levels and ERK1/2 activation in HEK293T cells transfected with HA-CXCR4-vYFP and myc-V2R pretreated or not with PD184352 for 30 min before stimulation with AVP for the indicated time. (*E*) CXCR4 cell-surface expression level in SupT1 cells treated or not with EGF for 15 min. In all cases, data shown represent the mean ± SEM of at least three independent experiments and are normalized to 100% of the control conditions. Total ERK1/2 and ERK1/2 activation status [(p)ERK1/2] were assessed by immunoblotting. $*P < 0.05$; $**P < 0.01$; $***P < 0.001$; NS, not significant.

β-Arrestin Phosphorylation Is Required for ERK/MAPK-Induced CXCR4 Redistribution. To determine if CXCR4 subcellular redistribution results from the direct phosphorylation of βarr2 by ERK1/2, we first tested if activated ERK1 could phosphorylate purified βarr2 and βarr1 in vitro. As shown in Fig. 6*D*, ERK1 induced a robust incorporation of [^{32}P] in both βarr1 and βarr2, with βarr2 appearing to be a better substrate. Quantification of ^{32}P incorporation revealed saturable phosphorylation with stoichiometry approaching 2 (mol/mol) for βarr1 and 2.5 for βarr2, consistent with the presence of at least two phosphorylation sites. We then analyzed phospho-βarr2 by MS to identify the ERK1 phosphorylation sites. MS/MS sequencing revealed the presence of βarr2-derived phosphopeptides containing Thr276 (Fig. S3*A*). This position corresponds to one of the potential ERK1/2 consensus sites (Ser/Thr-Pro) (44) in βarr2 (Ser14, Ser264, and Thr276) (Fig. S3*B*). Unphosphorylated peptides containing the other potential sites were detected at much lower abundance, but Ser14 had been identified previously as being phosphorylated in Jurkat cells (45). It should be noted that all putative sites are evolutionarily conserved in βarr2 (Fig. S3*C*), but only Ser14 and Thr276 are found in both βarr1 and βarr2 (Fig. S3*D*), underscoring the likelihood of their importance for βarr function. As shown in Fig. S3*B*, *in silico* analysis of residues' accessibility using molecular modeling of βarr2 from its crystal structure [Protein Data Bank (PDB) ID code 3P2D] with the Molecular Operating Environment software (MOE) (46) suggests that in the basal inactivated state Thr276 is exposed to the solvent and consequently could be easily accessible to protein kinases. In contrast, Ser14 is buried in the core of the protein and probably would require reorganization of the molecular environment to be phosphorylated.

To determine the role of βarr2 phosphorylation in ERK1/2-dependent GPCR regulation, Ser14, Ser264, and Thr276 were replaced individually by unphosphorylatable alanine residues (S14A, S264A, and T276A). Then these βarr2 mutants were tested for their ability to restore CXCR4 modulation upon ERK1/2 activation in βarr1/2-KO cells. As shown in Fig. 6*E*, in contrast to βarr2-WT or βarr2-S264A, the expression of βarr2-S14A or βarr2-T276A failed to restore any significant ERK1/2-promoted CXCR4 sequestration, suggesting that phosphorylation of both residues has a role in this mechanism. These results are supported further by the observation that the expression of a mutant form of βarr2 harboring phosphomimetic residues at positions Ser14 and Thr276 (S14D/T276D; S/T2D) was sufficient to decrease CXCR4 cell-surface localization in the absence of activation (Fig. 6*F*). Both S14A/T267A (S/T2A) and S/T2D βarr2 mutant forms maintained their ability to be recruited to CXCR4 upon activation of the receptor by its natural ligand CXCL12 (Fig. S4), confirming their functionality. Together, these results suggest that βarr2 phosphorylation at Ser14 and Thr276 via an ERK1/2-dependent mechanism promotes CXCR4 redistribution, thus dampening GPCR signaling.

Discussion

Our data demonstrate that ERK1/2 activation leads to the sequestration of GPCRs into intracellular vesicles, functionally resulting in the loss of cell responsiveness to GPCR stimulation. This phenomenon appears to be conserved among a subclass of GPCRs that recruit βarr2 in response to agonist activation. Indeed, our results show that ERK1/2 activation also affects the distribution of V2R and AT1R (43), but not FP, which undergoes endocytosis in a βarr-independent manner (42). Consistently, we found that receptor redistribution requires the phosphorylation of βarr2 by ERK1/2, unraveling an uncharacterized molecular mechanism for crosstalk between ERK1/2 and GPCR signaling.

The ERK1/2-dependent intracellular redistribution of GPCRs was observed in response to constitutive activation of the MAPK pathway (by active forms of MEK1 and H-Ras), stimulation of ERK1/2-activating GPCRs (V2R) or RTKs (EGFR), or pharmacological activation of the ERK/MAPK pathway (by PMA). Receptor

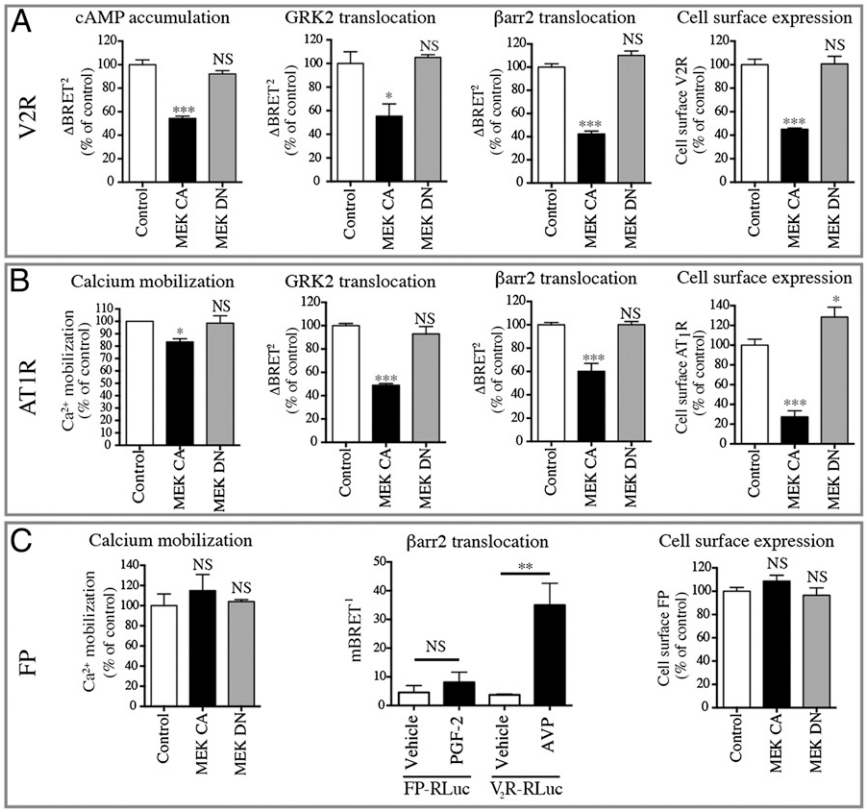

Fig. 5. Activation of the ERK/MAPK pathway blunts signaling by reducing the cell-surface expression of V2R and AT1R. cAMP accumulation (GFP10-EPAC-RLucII) (*A, Left*), calcium mobilization (Obelin-Cherry) (*B* and *C, Left*), GRK2 recruitment (GRK2-GFP10) (*A* and *B, Center Left*), and βarr2 recruitment (βarr2-GFP10) (*A* and *B, Center Right* and *C, Center*) were measured in HEK293T cells transfected with V2R (*A*), AT1R (*B*), or FP (*C*) along with the appropriate biosensors in the absence (Control) or presence of the indicated MEK mutants. Cellular activities were measured by BRET, as in Fig.1, after the addition of AVP (*A*), AngII (*B*), or PGF-2 (*C*). Cell-surface expression (*A–C, Right*) was measured by dual-flow cytometry in the absence of ligand stimulation as in Fig. 2. Data shown are the mean ± SEM of at least three independent experiments and were normalized to the control condition (100%).*$P < 0.05$; ***$P < 0.001$; NS, not significant.

sequestration resulted in a loss of cell responsiveness to GPCR agonists, as assessed by G-protein activation, second-messenger generation, and GRK and βarr recruitment. This phenomenon represents a heterologous desensitization process that had not been appreciated until now. Because many GPCRs activate ERK1/2, it could be hypothesized that this mechanism also contributes to the homologous desensitization of such receptors.

PKC activation with different phorbol esters, including PMA, was shown previously to promote the endocytosis of several GPCRs, including CXCR4 (47–49). These results have been attributed to a potential PKC-mediated phosphorylation of the receptor itself, but a direct link between receptor phosphorylation and its PMA-induced endocytosis had not been established. Our data demonstrate that PMA-stimulated CXCR4 endocytosis requires ERK1/2 activation, suggesting that the mechanism elucidated in the present study may explain the effect of PMA on the endocytosis of many GPCRs.

The ERK1/2-induced sequestration of GPCRs into cytoplasmic vesicles could result from either accelerated constitutive endocytosis or reduced recycling from endosomes to the plasma membrane. Given the classical role of βarr in the endocytosis process, the first possibility appears more likely. This idea is supported by the observation that ERK1/2 activation led to the sequestration of V2R, a receptor that does not undergo significant recycling following endocytosis (50). Whether the modulation of constitutive endocytosis results from an increased affinity of ERK1/2-phosphorylated βarrs for unliganded receptors or for other proteins involved in the endocytic process remains to be determined. Interestingly, one of the putative ERK1/2 phosphorylation sites identified in βarr2, Ser14, is located in close proximity to two lysine residues, Lys11 and Lys12. These lysines bind the phosphate moieties of the phosphorylated receptors and can facilitate the transition to the high-affinity receptor–βarr binding state (51). Therefore it could be hypothesized that the phosphorylation of Ser14 may mimic the phosphorylated receptor, thus promoting a high-affinity interaction with an inactive, nonphosphorylated receptor.

The causal link between ERK1/2 activation and steady-state receptor redistribution is supported by the complete inhibition of the PMA- and EGF-induced CXCR4 sequestration by the MEK1/2 inhibitor PD184352. Moreover, the kinetics of CXCR4 redistribution paralleled that of ERK1/2 activation, with both ERK1/2 activation and receptor sequestration being sustained for PMA but transient for EGF stimulation. The rescue experiments using nonphosphorylatable forms of human βarr2 or βarr2 harboring phosphomimetic residues further establishes the link between βarr2 phosphorylation and receptor sequestration. The lack of redistribution of FP, a receptor that cannot recruit βarr2, also is consistent with the central role of βarr2 in ERK1/2-promoted receptor relocalization.

Our results suggest the involvement of two putative ERK1/2 phosphorylation sites in βarr2, Ser14 and Thr276, because their mutation to alanine residues blocked ERK1/2-promoted CXCR4 sequestration, whereas their replacement by phosphomimetic aspartate residues mimicked the effect of ERK1/2 activation. One of these sites, Thr276, was confirmed to be a direct ERK1 phosphorylation site by our MS/MS analysis, whereas Ser14 previously had been shown to be phosphorylated in a large-scale phosphoproteomic study (45), thus supporting the notion that ERK1/2 phosphorylates βarr2 on these two residues. Although these phosphorylation sites are conserved in βarr1, whether βarr1 phosphorylation on these sites also contributes to receptor redistribution remains to be demonstrated directly. Using 2D tryptic phosphopeptide mapping, a previous study identified another serine residue, Ser412, as a direct ERK1/2 phosphorylation site in rat βarr1 (30). However, because Ser412 is not conserved in either rat or human βarr2, it is unlikely that this site plays any major role in the mechanisms described here. More recently, Ser178 was proposed as a phosphorylation site for ERK1/2 in rat βarr2 and was found to modulate the dynamics of

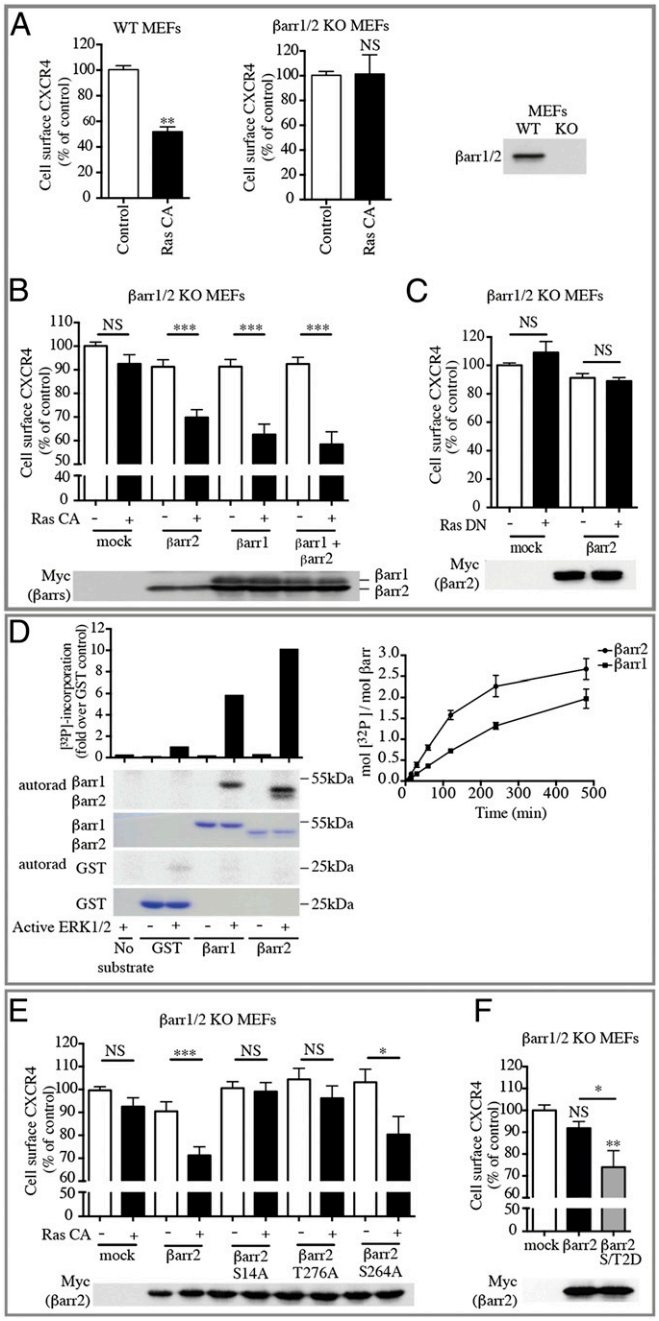

Fig. 6. ERK1/2-dependent βarr2 phosphorylation on S14 and T276 induces CXCR4 intracellular sequestration. (*A–C*) CXCR4 cell-surface expression was assessed by dual-flow cytometry in WT MEFs or βarr1/2-KO MEFs transiently transfected with HA-CXCR4-vYFP in the absence (Control) or presence of the indicated Ras mutants (*A*) and with or without βarr1 and/or βarr2 complementation (*B* and *C*). (*D*) Phosphorylation of βarrs was performed with recombinant bovine βarr1 or βarr2 as a substrate and recombinant active ERK1 in the presence of [γ^{32}P]-ATP for 15 min. The gel was stained with Coomassie, and ^{32}P incorporation was quantified using a PhosphorImager (*Left*) or during kinetics using scintillation counting (*Right*). The data shown are representative of three independent experiments. (*E* and *F*) CXCR4 cell-surface expression was assessed by dual-flow cytometry in βarr1/2-KO MEFs transiently transfected with HA-CXCR4-vYFP, βarr2 WT, or the indicated βarr2 mutants, with or without Ras CA. Data shown represent the mean ± SEM of at least three independent experiments and were normalized to the control condition (100%). Expression of βarr2 WT and mutants were assayed by immunoblotting. $*P < 0.05$; $**P < 0.01$; $***P < 0.001$; NS, not significant.

βarr2 within the endosomal compartment (31). However, this mechanism is distinct from the one we describe, because rat Ser178 is not conserved in human βarr2.

In the present study, we identified two phosphorylation sites for ERK1/2 in βarr2 that play a key role in regulating steady-state cell-surface expression of different GPCRs. Given the large proportion of GPCRs that interact with βarrs, the observed receptor sequestration promoted by the ERK1/2-mediated phosphorylation of βarr could have a major impact on the tonic regulation of cell responsiveness to a variety of hormonal stimulations. Because ERK1/2 activation is known to be deregulated in many pathological diseases, including several cancers, this mechanism could have far-reaching consequences for our understanding of different pathophysiological processes.

Materials and Methods

Plasmids. The following plasmids were described previously: Flag-MEK1-S218/222D (52), Gβ1 and GFP10-Gγ2 (53), CXCR4-RLucII (54), CXCR4-YFP (55), Obelin-Cherry (56), Gαi1-91RLucII, HA-CXCR4, and HA-CXCR4-vYFP (36), GFP10-EPAC-RLucII and HA-AT1R (57), HA-FP (58), and HA-V2R (59). HA-FP-vYFP and FP-RLucII were provided by Terrence Hébert, McGill University, Montreal. The βarr2-GFP10 construct was built by replacing the RLucII sequence from the previously published βarr2-RLucII (36). vYFP was introduced into pIRESP-HA to generate the pIRESP-HA-vYFP vector. The FP, V2R, or spAT1R (sp: signal peptide MKTIIALSYIFCLVFA at the N terminus) sequence was introduced into pIRESP-HA-vYFP to generate pIRESP-HA-FP-vYFP, pIRESP-HA-V2R-vYFP, or pIRESP-HA-AT1R-vYFP. Human βarr1 and βarr2 cDNA were obtained from the cDNA Resource Center and were cloned in pCMV-Tag3B (Stratagene) to obtain myc-tagged proteins, and H-Ras and MEK1 cDNA were cloned in pCMV-Tag2A (Stratagene) to obtain Flag-tagged proteins. All mutants (βarr2-S14A, -T126A, -S264A, -S/T2D; H-Ras-G12V, -S17N; and MEK1-K97A) were generated using the QuikChange (Stratagene) methodology and were verified by sequencing.

Reagents and Antibodies. CXCL12 was purchased from Cedarlane. Arginine vasopressin (AVP), PGF-2, and angiotensin II (AngII) were purchased from Sigma-Aldrich. A23187 was purchased from Tocris. The MEK1/2 inhibitor PD184352 was purchased from Selleck Chemicals. The ERK1/2 activators EGF and PMA were purchased from Invitrogen and Fisher Scientific, respectively. Anti-ERK1/2, anti–phospho-ERK1/2 (T202/Y204), and anti-βarr1/2 antibodies were purchased from Cell Signaling Technologies. Anti-myc and anti-Flag, antibodies were purchased from Sigma-Aldrich. Anti-human CXCR4 antibody was purchased from BioLegend. Anti-HA antibody (HA-11) was purchased from Covance. Anti-mouse Alexa Fluor 647 secondary antibody was purchased from Invitrogen. All secondary HRP-conjugated antibodies used for immunoblotting were purchased from Chemicon. All cell culture reagents were from Wisent.

Cell Culture. HEK293T, HeLa, βarr1/2-KO MEFs, and WT MEFs were cultured in DMEM supplemented with 10% (vol/vol) FBS, 100 IU/mL penicillin, and 100 μg/mL streptomycin. βarr1/2-KO mice were generated as described (43), and established MEF cultures were prepared according to the 3T3 protocol of Todaro and Green (60). For HEK293T HA-CXCR4-vYFP stable cell lines, a YFP$^+$ polyclonal cell population was obtained by flow cytometry cell sorting and was maintained in DMEM supplemented with 10% (vol/vol) FBS, 100 IU/mL penicillin, 100 μg/mL streptomycin, and 3 μg/mL puromycin. Sup-T1 cells were cultured in RPMI-1640 medium supplemented with 10% (vol/vol) FBS, 100 IU/mL penicillin, and 100 μg/mL streptomycin.

Transfections. The day before transfections, HEK293T or HEK293T HA-CXCR4-vYFP cells were seeded in six-well plates at a density of 600,000 cells per well. Transient transfections were performed using linear polyethylenimine 25 kDa (PEI) (Polysciences, Inc.) as transfection agent, at a PEI:DNA ratio of 3:1. Cells were maintained in culture for the next 48 h, and BRET experiments were carried out subsequently. For the transfection of MEFs, cells were seeded in six-well plates at a density of 600,000 cells per well and on the next day were transiently transfected using FuGENE HD (Promega), at a FuGENE HD:DNA ratio of 3:1. Cells were maintained in culture for the next 24 h, and FACS experiments were carried out subsequently.

BRET Assays. BRET assays were performed as described previously (36, 61). For BRET480-YFP, proteins were fused to RLuc as energy donor and YFP as acceptor. Coelenterazine-h (coel-h) (NanoLight Technology) was used as the luciferase substrate to generate light with a maximal emission peak at

480 nm, allowing YFP excitation (maximum at 488 nm). For BRET400-GFP10, proteins were fused to RLucII (donor) and GFP10 (acceptor). Coelenterazine-400a (coel-400a) (Biotium) was used as the luciferase substrate to generate light with a maximal emission peak at 400 nm, allowing GFP10 excitation (maximum at 400 nm). BRET was measured using a Mithras LB940 Multimode Microplate Reader (Berthold Technologies) equipped with either a BRET480-YFP filter set (donor 480 ± 20 nm and acceptor 530 ± 20 nm filters) or a BRET400-GFP10 filter set (donor 400 ± 70 nm and acceptor 515 ± 20 nm filters). Briefly, cells were seeded the day after transfection in a poly-L-ornithine (Sigma-Aldrich)–pretreated 96-well microplate (CulturePlate; PerkinElmer Inc.) and were starved overnight in DMEM for at least 8 h after seeding. The day of the experiment, cells were incubated with HBSS (Invitrogen) complemented with 0.1% BSA (HBSS/BSA) and stimulated with ligands (CXCL12: 200 nM; AVP: 100 nM; AngII: 1 μM; PGF-2: 1 μM) for 15 min. Where indicated, cells were pretreated with PD184352 (10 μM) for 30 min before stimulation with EGF (25 ng/mL) for 15 min or PMA (100 ng/mL) for 30 min (maximal response) or for the indicated times (time course). BRET values were collected after the addition of the luciferase substrate at a final concentration of 2.5 μM. BRET signals were determined as the ratio of the light emitted by acceptor (YFP or GFP10) over donor (RLuc or RLucII). The ligand-promoted BRET signal (ΔBRET) was calculated by subtracting the BRET values obtained in the vehicle condition from the values measured with ligand. ΔBRET was expressed as a percentage of the ΔBRET obtained in the control condition in which the ERK/MAPK pathway was not modulated by either a mutant or a treatment.

Calcium Measurements. HEK293T cells were transiently transfected with Obelin-Cherry used as a calcium reporter (34). The day after transfection, cells were seeded in a poly-L-ornithine–pretreated 96-well microplate to obtain duplicate plates for ligand or ionophore stimulation. The day of the experiment, cells were washed with HBSS and incubated for 2 h in the dark, at room temperature, with 1 μM coelenterazine cp (Biotium) diluted in HBSS/BSA. Luminescence measurements were recorded for 60 s on a FlexStation II (Molecular Devices) after ligand injection (CXCL12: 200 nM; A23187: 10 μM; AngII: 1 μM; PGF-2: 1 μM). Kinetics were normalized, setting the maximal response of the ligand at 100%. Bar graphs were generated from the area under the curve of each kinetic.

Flow Cytometry. Briefly, 48 h after transfection, HEK293T HA-CXCR4-vYFP cells were starved overnight in DMEM. Where indicated, cells were pretreated with PD184352 before EGF or PMA stimulation. Then the cells were rinsed with ice-cold HBSS and resuspended in HBSS/BSA. Cell-surface receptors were labeled on ice using a monoclonal anti-HA antibody followed by an anti-mouse Alexa Fluor 647 secondary antibody. SUP-T1 cells were starved overnight and then were stimulated with EGF for 15 min, rinsed with ice-cold HBSS, resuspended in HBSS containing Fc block solution 24G2 (anti-CD16/32-FcRγ), and stained using an anti-human CXCR4 antibody (PerCP/Cy5.5 anti-human CD184 clone 12G5; BioLegend) for 45 min on ice. Cells were washed, resuspended, and analyzed through an LSR II flow cytometer (BD Biosciences) set to detect YFP and Alexa Fluor 647 or PerCP/Cy5.5. Data analysis was performed using BD FACSDiva software.

Image Acquisition and Analysis. Briefly, HeLa cells were transfected and then seeded into a μ-Dish (IBIDI; no. 81156). Two days after transfection, epifluorescence confocal microscopy images from single confocal sections (0.7 μm) were acquired at room temperature with an LSM 510 Meta laser-scanning confocal microscope (Zeiss) using a Plan Apochromat 100× oil-immersion objective. All images were acquired using identical parameters. The colocalization between the membrane and the YFP signal was determined using ImageJ software (NIH). First, a line crossing a YFP^+ cell was drawn on the phase-contrast image, and the coordinates of the plasma membrane and the intracellular compartments were determined from the gray intensity profile along this line. Then the same line was transposed to the YFP image, and mean fluorescence intensity profiles along this line were obtained. Using the coordinates of the plasma membrane and the intracellular compartment, total YFP intensities were calculated, and both the plasma membrane and inner cell intensities were expressed as a percentage of total intensity along the section in each condition.

In Vitro Phosphorylation Assays. Phosphorylation assays were performed in vitro with recombinant bovine βarr1 or βarr2 (gift of Stéphane Laporte, McGill University, Montreal) as a substrate (3 μg per assay) and recombinant active ERK1 (100 ng per assay; Millipore; no. 14-439). The reaction products were subjected to SDS/PAGE, and ^{32}P incorporation was quantified using a Bio-Rad phosphorimager and MultiGauge software. To calculate the phosphate:substrate ratio, [^{32}P] incorporation in βarr1 or βarr2 was measured using a scintillation counter and was normalized to the specific activity of [^{32}P]ATP in the reaction.

Immunoblotting. Cell lysates were subjected to SDS/PAGE on 10% acrylamide gels and electroblotted to PVDF membranes. Blocking and primary and secondary antibody incubations of immunoblots were performed in Tris-buffered saline/Tween 20 [10 mM Tris (pH 7.4), 150 mM NaCl, and 0.1% Tween 20] supplemented with 5% (wt/vol) dry skim milk powder. The primary antibodies anti-HA, anti-myc, anti-Flag, anti–phospho-ERK1/2, and anti-βarr1/2 were used according to the manufacturers' instructions. HRP-conjugated donkey anti-rabbit and anti-mouse IgGs were used at a dilution of 1:5,000, and immunoreactive bands were detected using enhanced chemiluminescence.

Sample Preparation and Trypsin Digestion for LC-MS/MS. The gel slices were washed two times with 100% acetonitrile for 10 min and with H_2O for 20 min. Then the samples were dried using a speed vacuum. Proteins were reduced in 50 mM ammonium bicarbonate (pH 7.5) containing 10 mM DTT and were incubated for 1 h at 56 °C, followed by alkylation with 55 mM iodoacetamide for 1 h at 25 °C in the dark. The samples were washed and dried again as described above. Proteins were digested overnight with sequencing-grade modified trypsin (enzyme:protein ratio of 1:50) at 37 °C. Peptides from the gel slices were extracted using 100% acetonitrile. The samples were evaporated to dryness in a SpeedVac.

Liquid Chromatography and Nanoflow LC-MS/MS. Peptides were injected into a nanoflow HPLC system (Eksigent; Thermo Fisher Scientific) for online reversed-phase chromatographic separation. Peptides were loaded in a 5-mm-long trap column (i.d. 300 μm) in buffer A (0.2% formic acid) and were separated in an 18-cm-long fused silica capillary analytical column (i.d. 150 μm), both packed with 3-μm 200-Å Magic C18 AQ reverse-phase material (Michrom). Peptides were eluted by an increasing concentration of buffer B (0.2% formic acid in acetonitrile) from 5–40% over 100 min. After the gradient elution, the column was washed with 80% buffer B and re-equilibrated with 5% buffer B. Peptides were eluted into the mass spectrometer at a flow rate of 600 nL/min. The total run time was ∼70 min, including sample loading and column conditioning. Peptides were analyzed using an automated data-dependent acquisition on an LTQ-Orbitrap Elite or Q Exactive mass spectrometer. For LTQ-Orbitrap Elite analysis, each MS scan was acquired at a resolution of 240,000 FWHM (at 400 *m/z*) for mass range 300–2,000 with the lock mass option enabled (*m/z*: 445.120025) and was followed by up to 12 MS/MS data-dependent scans on the most intense ions using collision-induced activation (CID). Automatic gain control (AGC) target values for MS and MS/MS scans were set to 1e6 (maximum fill time, 500 ms) and 1e5 (maximum fill time, 50 ms), respectively. The precursor isolation window was set to 2 with CID normalized collision energy of 35; the dynamic exclusion window was set to 60 s. For Q Exactive analysis, each MS scan was acquired at a resolution of 70,000 FWHM (at *m/z* 200) for mass range 300–2,000, and the 12 most intense peaks were fragmented in the higher-energy collisional dissociation (HCD) collision cell with normalized collision energy of 25%. AGC target values for MS and MS/MS scans were set to 1e6, and the dynamic exclusion window was set to 15 s.

MS Data Acquisition. MS data were analyzed using Mascot Distiller software and were searched against the UniProtKB protein knowledgebase release 2014_11 database (www.expasy.org) containing 547,085 entries. For database searching, the enzyme specificity was set to trypsin with the maximum number of missed cleavages set to 2. The precursor mass tolerance was set to 10 ppm. Search criteria included a static modification of cysteine residues of +57.0214 Da, a variable modification of +15.9949 Da to include potential oxidation of methionines, and a modification of +79.966 on serine, threonine, or tyrosine for the identification of phosphorylation. Ion score cutoff and significance threshold *P* values were set to 25 and 0.05, respectively.

Data Analysis and Statistics. All graphs were generated and analyzed using GraphPad Prism (GraphPad Software Inc.). Data presented are the means ± SEM of a least three independent experiments. Statistical analysis was performed using either a paired Student's *t* test when two values were compared or one-way ANOVA with Dunnett's post hoc test when more than two values were compared with the control. $*P < 0.05$, $**P < 0.01$, $***P < 0.001$.

ACKNOWLEDGMENTS. We thank Monique Lagacé for critical reading of the manuscript; Stéphane Laporte for providing recombinant βarr1/2; Martin Audet and Viktoriya Lukashova from the M.B. laboratory and Darlène Pétrin and Eugénie Goupil from Terrence Hébert's laboratory for providing pIRESP-HA-V2R-vYFP

and pIRESP-HA-AT1R-vYFP and HA-FP-vYFP and FP-RLucII plasmids, respectively; and Dr. Robert Lefkowitz for providing βarr1/2-KO MEFs. This work was supported by Canadian Institutes of Health Research Grants MOP10501 (to M.B.) and MOP123408 (to P.P.R.), a grant from the Human Frontier Science Program (to P.P.R.), a grant from the Cancer Research Foundation France (ARC) (to M.G.H.S.), grants from the Ligue Contre le Cancer Comité de l'Oise (to H.E. and M.G.H.S.), and a grant from the Fondation pour la Recherche Médicale (to S.M.). M.B. holds a Canada Research Chair in Signal Transduction and Molecular Pharmacology. P.P.R. holds Canada Research Chair in Cell Signaling and Proteomics.

1. Seger R, Krebs EG (1995) The MAPK signaling cascade. *FASEB J* 9(9):726–735.
2. Roskoski R, Jr (2012) ERK1/2 MAP kinases: Structure, function, and regulation. *Pharmacol Res* 66(2):105–143.
3. Schlessinger J (2002) Ligand-induced, receptor-mediated dimerization and activation of EGF receptor. *Cell* 110(6):669–672.
4. McKay MM, Morrison DK (2007) Integrating signals from RTKs to ERK/MAPK. *Oncogene* 26(22):3113–3121.
5. Marinissen MJ, Gutkind JS (2001) G-protein-coupled receptors and signaling networks: Emerging paradigms. *Trends Pharmacol Sci* 22(7):368–376.
6. Delcourt N, Bockaert J, Marin P (2007) GPCR-jacking: From a new route in RTK signalling to a new concept in GPCR activation. *Trends Pharmacol Sci* 28(12):602–607.
7. Kolch W, et al. (1993) Protein kinase C alpha activates RAF-1 by direct phosphorylation. *Nature* 364(6434):249–252.
8. Koch WJ, Hawes BE, Allen LF, Lefkowitz RJ (1994) Direct evidence that Gi-coupled receptor stimulation of mitogen-activated protein kinase is mediated by G beta gamma activation of p21ras. *Proc Natl Acad Sci USA* 91(26):12706–12710.
9. Crespo P, Xu N, Simonds WF, Gutkind JS (1994) Ras-dependent activation of MAP kinase pathway mediated by G-protein beta gamma subunits. *Nature* 369(6479): 418–420.
10. Lev S, et al. (1995) Protein tyrosine kinase PYK2 involved in Ca(2+)-induced regulation of ion channel and MAP kinase functions. *Nature* 376(6543):737–745.
11. Lopez-Ilasaca M, Crespo P, Pellici PG, Gutkind JS, Wetzker R (1997) Linkage of G protein-coupled receptors to the MAPK signaling pathway through PI 3-kinase gamma. *Science* 275(5298):394–397.
12. Luttrell LM, et al. (1999) Beta-arrestin-dependent formation of beta2 adrenergic receptor-Src protein kinase complexes. *Science* 283(5402):655–661.
13. DeFea KA, et al. (2000) beta-arrestin-dependent endocytosis of proteinase-activated receptor 2 is required for intracellular targeting of activated ERK1/2. *J Cell Biol* 148(6): 1267–1281.
14. Luttrell LM, Gesty-Palmer D (2010) Beyond desensitization: Physiological relevance of arrestin-dependent signaling. *Pharmacol Rev* 62(2):305–330.
15. Daub H, Weiss FU, Wallasch C, Ullrich A (1996) Role of transactivation of the EGF receptor in signalling by G-protein-coupled receptors. *Nature* 379(6565):557–560.
16. Noma T, et al. (2007) Beta-arrestin-mediated beta1-adrenergic receptor transactivation of the EGFR confers cardioprotection. *J Clin Invest* 117(9):2445–2458.
17. Galet C, Ascoli M (2008) Arrestin-3 is essential for the activation of Fyn by the luteinizing hormone receptor (LHR) in MA-10 cells. *Cell Signal* 20(10):1822–1829.
18. Hupfeld CJ, Olefsky JM (2007) Regulation of receptor tyrosine kinase signaling by GRKs and beta-arrestins. *Annu Rev Physiol* 69:561–577.
19. Lin FT, Daaka Y, Lefkowitz RJ (1998) beta-arrestins regulate mitogenic signaling and clathrin-mediated endocytosis of the insulin-like growth factor I receptor. *J Biol Chem* 273(48):31640–31643.
20. Oligny-Longpré G, et al. (2012) Engagement of β-arrestin by transactivated insulin-like growth factor receptor is needed for V2 vasopressin receptor-stimulated ERK1/2 activation. *Proc Natl Acad Sci USA* 109(17):E1028–E1037.
21. Dalle S, Ricketts W, Imamura T, Vollenweider P, Olefsky JM (2001) Insulin and insulin-like growth factor I receptors utilize different G protein signaling components. *J Biol Chem* 276(19):15688–15695.
22. Hinney A, et al. (2003) Melanocortin-4 receptor gene: Case-control study and transmission disequilibrium test confirm that functionally relevant mutations are compatible with a major gene effect for extreme obesity. *J Clin Endocrinol Metab* 88(9): 4258–4267.
23. Kim J, Ahn S, Guo R, Daaka Y (2003) Regulation of epidermal growth factor receptor internalization by G protein-coupled receptors. *Biochemistry* 42(10):2887–2894.
24. Hollenberg MD (1995) Tyrosine kinase-mediated signal transduction pathways and the actions of polypeptide growth factors and G-protein-coupled agonists in smooth muscle. *Mol Cell Biochem* 149-150:77–85.
25. Benovic JL, Strasser RH, Caron MG, Lefkowitz RJ (1986) Beta-adrenergic receptor kinase: Identification of a novel protein kinase that phosphorylates the agonist-occupied form of the receptor. *Proc Natl Acad Sci USA* 83(9):2797–2801.
26. Pitcher JA, Freedman NJ, Lefkowitz RJ (1998) G protein-coupled receptor kinases. *Annu Rev Biochem* 67:653–692.
27. Bouvier M, et al. (1988) Removal of phosphorylation sites from the beta 2-adrenergic receptor delays onset of agonist-promoted desensitization. *Nature* 333(6171):370–373.
28. Benovic JL, et al. (1985) Phosphorylation of the mammalian beta-adrenergic receptor by cyclic AMP-dependent protein kinase. Regulation of the rate of receptor phosphorylation and dephosphorylation by agonist occupancy and effects on coupling of the receptor to the stimulatory guanine nucleotide regulatory protein. *J Biol Chem* 260(11):7094–7101.
29. Hausdorff WP, et al. (1989) Phosphorylation sites on two domains of the beta 2-adrenergic receptor are involved in distinct pathways of receptor desensitization. *J Biol Chem* 264(21):12657–12665.
30. Lin FT, Miller WE, Luttrell LM, Lefkowitz RJ (1999) Feedback regulation of beta-arrestin1 function by extracellular signal-regulated kinases. *J Biol Chem* 274(23):15971–15974.
31. Khoury E, Nikolajev L, Simaan M, Namkung Y, Laporte SA (2014) Differential regulation of endosomal GPCR/β-arrestin complexes and trafficking by MAPK. *J Biol Chem* 289(34):23302–23317.
32. Galés C, et al. (2006) Probing the activation-promoted structural rearrangements in preassembled receptor-G protein complexes. *Nat Struct Mol Biol* 13(9):778–786.
33. Carrière A, et al. (2008) Oncogenic MAPK signaling stimulates mTORC1 activity by promoting RSK-mediated raptor phosphorylation. *Curr Biol* 18(17):1269–1277.
34. Campbell AK, Dormer RL (1975) Studies on free calcium inside pigeon erythrocyte 'ghosts' by using the calcium-activated luminescent protein, obelin. *Biochem Soc Trans* 3(5):709–711.
35. Vila-Coro AJ, et al. (1999) The chemokine SDF-1alpha triggers CXCR4 receptor dimerization and activates the JAK/STAT pathway. *FASEB J* 13(13):1699–1710.
36. Quoyer J, et al. (2013) Pepducin targeting the C-X-C chemokine receptor type 4 acts as a biased agonist favoring activation of the inhibitory G protein. *Proc Natl Acad Sci USA* 110(52):E5088–E5097.
37. Schneider CA, Rasband WS, Eliceiri KW (2012) NIH Image to ImageJ: 25 years of image analysis. *Nat Methods* 9(7):671–675.
38. Minden A, et al. (1994) Differential activation of ERK and JNK mitogen-activated protein kinases by Raf-1 and MEKK. *Science* 266(5191):1719–1723.
39. Frost JA, Geppert TD, Cobb MH, Feramisco JR (1994) A requirement for extracellular signal-regulated kinase (ERK) function in the activation of AP-1 by Ha-Ras, phorbol 12-myristate 13-acetate, and serum. *Proc Natl Acad Sci USA* 91(9):3844–3848.
40. Charest PG, Oligny-Longpré G, Bonin H, Azzi M, Bouvier M (2007) The V2 vasopressin receptor stimulates ERK1/2 activity independently of heterotrimeric G protein signalling. *Cell Signal* 19(1):32–41.
41. English JM, Cobb MH (2002) Pharmacological inhibitors of MAPK pathways. *Trends Pharmacol Sci* 23(1):40–45.
42. Goupil E, et al. (2012) Biasing the prostaglandin F2α receptor responses toward EGFR-dependent transactivation of MAPK. *Mol Endocrinol* 26(7):1189–1202.
43. Kohout TA, Lin FS, Perry SJ, Conner DA, Lefkowitz RJ (2001) beta-Arrestin 1 and 2 differentially regulate heptahelical receptor signaling and trafficking. *Proc Natl Acad Sci USA* 98(4):1601–1606.
44. Roux PP, Ballif BA, Anjum R, Gygi SP, Blenis J (2004) Tumor-promoting phorbol esters and activated Ras inactivate the tuberous sclerosis tumor suppressor complex via p90 ribosomal S6 kinase. *Proc Natl Acad Sci USA* 101(37):13489–13494.
45. Hornbeck PV, et al. (2012) PhosphoSitePlus: A comprehensive resource for investigating the structure and function of experimentally determined post-translational modifications in man and mouse. *Nucleic Acids Res* 40(Database issue): D261–D270.
46. 2014, C.C.G.I. Molecular Operating Environment (MOE) software. Available at www.chemcomp.com. Accessed July 30, 2015.
47. Signoret N, et al. (1997) Phorbol esters and SDF-1 induce rapid endocytosis and down modulation of the chemokine receptor CXCR4. *J Cell Biol* 139(3):651–664.
48. Liles WC, Hunter DD, Meier KE, Nathanson NM (1986) Activation of protein kinase C induces rapid internalization and subsequent degradation of muscarinic acetylcholine receptors in neuroblastoma cells. *J Biol Chem* 261(12):5307–5313.
49. Kelleher DJ, Pessin JE, Ruoho AE, Johnson GL (1984) Phorbol ester induces desensitization of adenylate cyclase and phosphorylation of the beta-adrenergic receptor in turkey erythrocytes. *Proc Natl Acad Sci USA* 81(14):4316–4320.
50. Innamorati G, Sadeghi HM, Tran NT, Birnbaumer M (1998) A serine cluster prevents recycling of the V2 vasopressin receptor. *Proc Natl Acad Sci USA* 95(5):2222–2226.
51. Gimenez LE, et al. (2012) Role of receptor-attached phosphates in binding of visual and non-visual arrestins to G protein-coupled receptors. *J Biol Chem* 287(12):9028–9040.
52. Carriere A, et al. (2011) ERK1/2 phosphorylate Raptor to promote Ras-dependent activation of mTOR complex 1 (mTORC1). *J Biol Chem* 286(1):567–577.
53. Galés C, et al. (2005) Real-time monitoring of receptor and G-protein interactions in living cells. *Nat Methods* 2(3):177–184.
54. Busillo JM, et al. (2010) Site-specific phosphorylation of CXCR4 is dynamically regulated by multiple kinases and results in differential modulation of CXCR4 signaling. *J Biol Chem* 285(10):7805–7817.
55. Percherancier Y, et al. (2005) Bioluminescence resonance energy transfer reveals ligand-induced conformational changes in CXCR4 homo- and heterodimers. *J Biol Chem* 280(11):9895–9903.
56. van der Westhuizen ET, Breton B, Christopoulos A, Bouvier M (2014) Quantification of ligand bias for clinically relevant β2-adrenergic receptor ligands: Implications for drug taxonomy. *Mol Pharmacol* 85(3):492–509.
57. Zimmerman B, et al. (2012) Differential β-arrestin-dependent conformational signaling and cellular responses revealed by angiotensin analogs. *Sci Signal* 5(221):ra33.
58. Goupil E, et al. (2010) A novel biased allosteric compound inhibitor of parturition selectively impedes the prostaglandin F2alpha-mediated Rho/ROCK signaling pathway. *J Biol Chem* 285(33):25624–25636.
59. Oakley RH, Laporte SA, Holt JA, Caron MG, Barak LS (2000) Differential affinities of visual arrestin, beta arrestin1, and beta arrestin2 for G protein-coupled receptors delineate two major classes of receptors. *J Biol Chem* 275(22):17201–17210.
60. Todaro GJ, Green H (1963) Quantitative studies of the growth of mouse embryo cells in culture and their development into established lines. *J Cell Biol* 17:299–313.
61. Mercier JF, Salahpour A, Angers S, Breit A, Bouvier M (2002) Quantitative assessment of beta 1- and beta 2-adrenergic receptor homo- and heterodimerization by bioluminescence resonance energy transfer. *J Biol Chem* 277(47):44925–44931.